the bond is broken, and resonance between these configurations is important. In this case we refine the GVB-RCI(2/4) description of these two pairs by using the GVB-CI(2/4) description, where all four electrons are allowed to occupy all four orbitals in any way (leading to 19 orbital products).

We find (see Figure 11) for Ni, Pd, and Pt that the GVB description (which uses 10 optimized orbitals for all states) leads to a rather accurate description of the relative energies for the d^{10}, s^1d^9, and s^2d^8 configurations and is particularly accurate for s^1d^9 vs. d^{10}, the states relevant for this paper. For the s^2d^8 states the s^2 pair was polarized in the $\pm z$ directions, and d_{z^2} and the d_{xy} were singly occupied.

For the various $M(R_1)(R_2)$ complexes, it is necessary to correlate not only the 10 metal valence electrons but also the additional electrons involved in the covalent $M-R_1$ and $M-R_2$ bonds. Thus, a total of 12 electrons or 6 electron pairs must be correlated. Consequently, we first carried out GVB-PP(6/12) calculations using 12 orbitals to correlate the motions of these 6 pairs (12 electrons). (All other orbitals are doubly occupied but are solved self-consistently.) In order to include the spin-coupling, interpair correlation, and resonance effects,[2a,c] the energetics reported here were determined at the GVB-CI(2/4) × RCI(4/8) level.

In *previous studies* of the reaction path for reductive coupling, the necessity for the simultaneous description of both the reactant (s^1d^9) and the product (d^{10}) resonance structures in the transition-state region required the use of three orbitals (rather than two) for each of the two bond pairs that change during the reaction.[2] Thus, rather than GVB-PP(2/4), these two electron pairs were described with GVB-PP(2/6). In order to allow a full description of resonance effects in the transition state, all occupations of these six orbitals were allowed for all four electrons, denoted as GVB-CI(2/6). The other four pairs of electrons were correlated as usual, leading to a composite wave function of the form GVB-CI(2/6) × RCI(4/8). We also optimized the orbitals at this level. In the *current study*, the main interest is in overall energy differences between products and reactants, where this resonance is not so important. Consequently, we use only two orbitals for these bond pairs, and the orbitals were optimized at the GVB-PP level. However, as in the previous studies, we carry out a full CI among the (four) orbitals involving those two bond pairs (CI(2/4)). Thus the wave function used in these studies is GVB-CI(2/4) × RCI(4/8).

Acknowledgment. This work was supported in part by a grant from the National Science Foundation (No. CHE83-18041). J.J.L. acknowledges financial support in the form of fellowships from Exxon and ARCO.

Registry No. 1, 79232-18-1; **2**, 79218-06-7; **3**, 103191-78-2; **4**, 79329-16-1; **5**, 79232-17-0; **6**, 76832-29-6; **7**, 76830-85-8; **8**, 78452-79-6.

Supplementary Material Available: Cartesian coordinates for Pt- and $Pd(CH_3)_2(PH_3)_2$, $PtCl_2(CH_3)_2(PH_3)_2$, $PtCl_2(PH_3)_2$, $Pt(H)(CH_3)(PH_3)_2$, and Pt- and $Pd(PH_3)_2$ and internal coordinates of methyls and phosphines (8 pages). Ordering information given on any current masthead page.

Ribose Puckering: Structure, Dynamics, Energetics, and the Pseudorotation Cycle

Stephen C. Harvey* and M. Prabhakaran

Contribution from the Department of Biochemistry, The University of Alabama at Birmingham, Birmingham, Alabama 35294. *Received October 2, 1985*

Abstract: We have examined the pucker dependence of ribose structure and ribose conformational energy in a set of 4800 configurations generated during a 304-K, 24-ps, in vacuo molecular dynamics simulation of phenylalanine transfer RNA. This data set spans all of the thermodynamically accessible regions of the northern (N), eastern (E), and southern (S) quadrants of the traditional polar representation of sugar pucker conformational space. Spontaneous repuckering, with passage between the minimum energy configurations at C2′-endo (S) and C3′-endo (N), occurs for riboses in single-stranded and loop regions with an observed frequency of about 1 ns^{-1}, and the lowest energy barrier is observed at O4′-endo, so repuckering is via the N–E–S pathway, as expected. The pseudorotational description of sugar pucker is found to be reasonably accurate, although we find a small dependence of pucker amplitude (θ_m) on pucker phase angle (P), and there are substantial fluctuations in θ_m at any given value of P. The three pseudorotation formalisms (Altona–Sundaralingam, Rao–Westhof–Sundaralingam, and Cremer–Pople) give only small differences when characterizing a given configuration, and we discuss relationships for interconverting between the formalisms. On examining our potential energy function, we find that the most important contributions to the shape of the conformational energy curve arise from the torsional energy terms. For examining questions of structure and for comparing different potential energy functions, molecular dynamics is a useful complement to energy minimization, because of the very large number of configurations that are generated, and because these configurations represent all thermally accessible states.

The central role of the furanose ring in the conformation of nucleic acids has long been recognized. The global conformation of the molecule is affected by sugar conformation in two ways. First, the backbone which connects successive phosphate atoms passes through the furanose ring. Second, the base is covalently bonded to the C1′ atom in the ring. Thus, the geometry of the sugar (ribose in RNAs, deoxyribose in DNAs) is one of the critical factors for determining the overall molecular architecture. It is also likely that changes in the conformation of sugars will play a fundamental role in the dynamic aspects of nucleic acid structures, a subject of increasing interest.

One of the most important features of furanose conformation is the sugar pucker, which arises because the five-membered ring would be highly strained if it were held in a planar configuration. A number of methods to mathematically describe the deviation of closed cyclic rings from planarity have been given.[1-5] Although their details differ (see Methods), they all describe the ring conformation in terms of a puckering phase angle, P, identifying which part of the ring is farthest from planarity, and an amplitude, measuring the magnitude of the deviation from planarity. Amplitude is denoted θ_m if pucker is defined in terms of ring torsion

(1) Kilpatrick, J. E.; Pitzer, K. S.; Spitzer, R. *J. Am. Chem. Soc.* **1947**, *69*, 2483–2488.
(2) Geise, H. J.; Altona, C.; Romers, C. *Tetrahedron Lett.* **1967**, *15*, 1383–1386.
(3) Altona, C.; Sundaralingam, M. *J. Am. Chem. Soc.* **1972**, *94*, 8205–8212.
(4) Cremer, D.; Pople, J. A. *J. Am. Chem. Soc.* **1975**, *97*, 1354–1358.
(5) Rao, S. T.; Westhof, E.; Sundaralingam, M. *Acta Crystallogr., Sect. A: Found. Crystallogr.* **1981**, *37*, 421–425.

0002-7863/86/1508-6128$01.50/0

angle[2,3] or q if it is defined in terms of atomic displacements from a reference plane.[1,4] We will use both the (P,θ_m) and (P,q) notations in this paper.

It is well known that the energy of cyclopentane and related compounds depends strongly upon puckering amplitude but is relatively independent of P. For this reason, it was suggested that conformational changes in these ring systems would take place along a pathway with a nearly constant nonzero value of puckering amplitude, the so called pseudorotation pathway.[1,3] The ribose ring has five atoms, each of which can be either above or below the plane at different stages of the pseudorotation cycle, so there will be 10 envelope (E) conformations, corresponding to P = 0, 36, 72°, ..., alternating with 10 twist (T) conformations, with P = 18, 54, 90°, ... The pseudorotation pathway can be thought of as a mechanism for passing deviations from planarity around the ring. Given a starting conformation, an increase of 360° in P takes us completely around the psuedorotation cycle, returning to the starting configuration.

It is customary to represent sugar pucker in two-dimensional polar plots, with the amplitude as the radial coordinate and the phase angle as the angular coordinate. In such a plot, the psuedorotation pathway would be a circle. Traditionally, P = 0° is placed at the top of the polar plot, with increasing values of P clockwise. With this representation, the crystallographically observed values of pucker for most nucleosides, nucleotides, and nucleic acids lie in the right-hand half of the polar plot, with the sugar pucker characteristic of RNA and A-DNA in the northern (N) quadrant, and the sugar pucker characteristic of B-DNA in the southern (S) quadrant. To get from the A-DNA to the B-DNA configuration along the pseudorotation pathway, it is generally believed that puckering proceeds via the O4′-endo configuration (N–E–S) rather than via the O4′-exo configuration (N–W–S), because of the unfavorable conformational energy of the latter.

A number of studies have attempted to determine the dependence of structural features and conformational energy on sugar pucker amplitude and phase angle.[3-12] Generally, model conformations have been constructed using fixed bond lengths, and the energy has been calculated from semiempirical energy functions. In one such study, Levitt and Warshel[6] concluded that the energy barrier between the C2′-endo and the C3′-endo configurations was only 0.5 kcal/mol, so that the furanose ring could be very easily deformed. This conclusion was disputed by Westhof and Sundaralingam,[7] for two reasons. First, the relaxed ribose geometries of Levitt and Warshel[6] had valence bond angles 5–6° larger than values expected from an analysis of numerous crystallographic structures. Second, an activation free energy of 4.7 ± 0.5 kcal/mol for repuckering between the C2′-endo and C3′-endo domains had been determined in a series of ^{13}C NMR relaxation experiments.[8,9] The idea that the ribose ring can repucker freely[6] was also contested by Olson and Sussman,[10] based on a statistical analysis of the distributions of solid-state puckerings observed in crystallographic studies and on a survey of NMR measurements of vicinal coupling constants in RNA and DNA analogues. A careful analysis of the experimental results led them to conclude that the pseudorotation barrier in furanose rings would be on the order of 2–5 kcal/mol. Olson, in a companion paper,[11] proposed a revised potential energy function that would more closely match the experimentally observed dependence of energy on pucker angle. In addition to the usual terms to account for the energies associated with bond lengths, bond angles, torsional rotations about bonds, and the nonbonded interactions, Olson's potential included a term for the so-called gauche effect, which is the tendency of certain sequences of atoms to prefer gauche over trans or cis torsional conformations. More recently, Weiner et al. have proposed a unified force field for conformational energy calculations on nucleic acids and proteins.[12] They find a dependence of energy on pucker angle similar to Olson's, in part due to a small modification of the electrostatic part of the nonbonded interactions.

There is one possible shortcoming to the studies described in the previous paragraph. Sugar pucker has been described with only two parameters (phase and amplitude), although the furanose ring, with five atoms, has $3N - 6 = 9$ internal degrees of freedom. In the previous studies,[3-7,10-12] a single conformation was chosen for analysis at each value of phase and amplitude, although each point in (P,q) space actually corresponds to an infinite number of furanose conformations, and therefore to an unknown range of structures and conformational energies. It is not immediately clear what effects are produced by this reduction in the number of degrees of freedom. In particular, since the structures of the earlier studies have often been optimized by energy minimization,[6,7,11,12] which effectively takes the structures to conformations characteristic of very low temperatures, it is possible that the resulting structures and energy profiles have errors arising from the failure to include the effects of dynamic averaging over the multitude of configurations that would occur at room temperature.

Our recent molecular dynamics simulation on tRNA[13-16] provides a new opportunity for examining the structure, dynamics, and energetics of sugar puckering. In the crystallographic structure the 76 riboses show a wide range of sugar puckers, and during the course of the simulation a substantial portion of (P,q) space is sampled by the fluctuations in pucker and by the spontaneous repuckering of two of the riboses. The simulation produces a very large number of structures for statistical analysis, which allows us to examine a variety of questions. First are the kinetic questions: How often does repuckering between the N and S hemispheres occur? What is the time scale of repuckering? Second are the questions related to the various formalisms that are used to describe sugar pucker: How large are the differences in pucker phase angle and amplitude when they are defined by the different formalisms? For a given point in (P,q) space, how large are the fluctuations in other structural parameters? Third are the structural questions: How closely is the pseudorotational pathway followed? How do bond lengths, valence angles, and endocyclic torsion angles vary with pucker? Fourth are the energetic questions: For our set of energy parameters, what is the dependence of the mean value of the conformational energy on P, the pucker phase angle? At a given value of P, how large are the fluctuations in conformational energy resulting from the thermal fluctuations in conformation?

This paper addresses the foregoing questions.

Methods

Definitions of Puckering Parameters. There are three different formalisms in common use for calculating pucker amplitudes and phase angles. The original Altona and Sundaralingam method[3] starts with the suggestion[17] that the five ribose torsion angles can, on the pseudorotation pathway, be described by a simple cosine function,

$$\theta_j = \theta_m \cos (P + 4\pi j/5) \qquad (1)$$

where j = 0–4, θ_m is the maximum torsional angle (typically on the order of 40°), and P is the pucker phase angle. The ribose torsion angles are identified as follows: θ_0 about C2′–C3′; θ_1 about

(6) Levitt, M.; Warshel, A. *J. Am. Chem. Soc.* **1978**, *100*, 2607–2613.
(7) Westhof, E.; Sundaralingam, M. *J. Am. Chem. Soc.* **1980**, *102*, 1493–1500.
(8) Roder, O.; Ludemann, H.-D.; Von Goldammer, E. *Eur. J. Biochem.* **1975**, *53*, 517–524.
(9) Ludemann, H.-D.; Westhof, E. In *Nuclear Magnetic Resonance Spectroscopy in Molecular Biology*; Pullman, B., Ed.; D. Reidel: Dordrecht, Holland, 1978; pp 1141–51.
(10) Olson, W. K.; Sussman, J. L. *J. Am. Chem. Soc.* **1982**, *104*, 270–278.
(11) Olson, W. K. *J. Am. Chem. Soc.* **1982**, *104*, 278–286.
(12) Weiner, S. J.; Kollman, P. A.; Case, D. A.; Singh, U. C.; Ghio, C.; Alagona, G.; Profeta, S.; Weiner, P. *J. Am. Chem. Soc.* **1984**, *106*, 765–784.
(13) Prabhakaran, M.; Harvey, S. C.; Mao, B.; McCammon, J. A. *J. Biomolec. Struct. Dynamics* **1983**, *1*, 357–369.
(14) Harvey, S. C.; Prabhakaran, M.; Mao, B.; McCammon, J. A. *Science* **1984**, *223*, 1189–1191.
(15) Harvey, S. C.; Prabhakaran, M.; McCammon, J. A. *Biopolymers* **1985**, *24*, 1169–1188.
(16) Prabhakaran, M.; Harvey, S. C.; McCammon, J. A. *Biopolymers* **1985**, *24*, 1189-1204.
(17) Altona, C.; Geise, H. J.; Romers, C. *Tetrahedron* **1968**, *24*, 13.

C3′–C4′; ...; θ_4 about C1′–C2′. A simple expression for P can be derived[17] from eq 1:

$$\tan P = \frac{(\theta_2 + \theta_4) - (\theta_1 + \theta_3)}{2\theta_0(\sin(\pi/5) + \sin(2\pi/5))} \quad (2)$$

Since eq 2 does not treat all five ring torsions identically, there is a small dependence of θ_m (eq 1) on the choice of a reference atom (in this case O4′, which is the atom opposite θ_0). To overcome this, a slightly different definition for θ_m and P was put forward by Rao, Westhof, and Sundaralingam,[5] based on an approximate Fourier analysis of the five ring torsions. If we define the Fourier sums

$$A = \theta_m \cos P = (2/5)\sum\theta_j \cos \alpha_j$$

$$B = \theta_m \sin P = -(2/5)\sum\theta_j \sin \alpha_j$$

where $\alpha_j = 4\pi j/5$ and the sums are taken from $j = 0$ to $j = 4$, then

$$\theta_m^2 = A^2 + B^2 \quad (3)$$

$$\tan P = B/A \quad (4)$$

Instead of defining the pucker amplitude in terms of the deviations of torsion angles from zero, it can be defined in terms of the distance of each atom from a suitable ring reference plane. This approach was developed by Cremer and Pople,[4] who chose a reference plane suitable to a Fourier analysis like that outlined above. The reference plane is not a best fit plane in the least-squares sense, but it is easy to calculate z_j, the distance of the jth atom from the Cremer–Pople plane, using simple expressions.[4] The pucker amplitude q (in Å) and the phase angle P are found by defining

$$C = q \cos P = (2/5)^{1/2}\sum z_j \cos \alpha_j$$

$$D = q \sin P = -(2/5)^{1/2}\sum z_j \sin \alpha_j$$

where $\alpha_j = 4\pi j/5$. With these definitions,

$$q^2 = C^2 + D^2 \quad (5)$$

$$P = \tan^{-1}(D/C) + \pi/2 \quad (6)$$

In this formalism, atoms 0 through 4 are taken to be O4′, C1′, C2′, C3′, C4′, so that the zero value of P corresponds to the same C2′–C3′ twist configuration ($^3_2$T) of the other two formalisms. (The factor of $\pi/2$ in eq 6 is not given in the original Cremer–Pople description, but it is necessary if we want the zero phase angle to be at the $^3_2$T configuration.)

Note that there are three slightly different definitions for P (eq 2, 4, and 6), but, for a number of crystallographic conformations, they all give values within 3° of one another.[5,18] The two definitions of θ_m (eq 1 and 3) also give similar values for a given conformation. For very small deviations from planarity, θ_m (as defined by eq 3) and q can be shown[19] to satisfy

$$\theta_m \text{ (deg)} = 102.5q \text{ (Å)} \quad (7)$$

a relationship that remains approximately true for larger pucker amplitudes; for a variety of crystal structures, errors in this expression are less than 6% for riboses and deoxyriboses.[5]

In this paper, we will refer to these formalisms as AS (Altona and Sundaralingam,[3] eq 1 and 2), RWS (Rao, Westhof, and Sundaralingam,[5] eq 3 and 4), and CP (Cremer and Pople,[4] eq 5 and 6), respectively. When we refer to the torsion angle definition of pucker amplitude, i.e., when discussing pucker in terms of (P,θ_m) space, we are using the AS formalism, unless otherwise indicated. In references to the pucker in (P,q) space, we are talking about the CP formalism.

Data Base. The structures used in this study were taken from our 24-ps in vacuo molecular dynamics simulation on tRNA^{Phe}; the details of that simulation and the parameters for the potential energy function are presented elsewhere.[15] It is, perhaps, worth repeating that we used the extended atom representation, without including explicit hydrogen atoms. Conventional parameters were used for the nonbonded interactions, with full, unscaled van der Waals and electrostatic terms for the 1–4 interactions. Solvent and the effects of counterion condensation were mimicked by scaling partial electrostatic charges on the five atoms of the phosphate groups to give a net charge of 0.2 e per residue (where e is the charge on the electron), and by using a distance-dependent dielectric constant that is numerically equal to the distance (in angstroms) between each pair of charges in the Coulombic electrostatic term in the potential function.

Table I. Mean, Standard Deviation, and Range of Pucker Angles of Riboses Used in This Study[a]

nucleotide	$\bar{P}$	σ_P	P_{min}	P_{max}
m^{2}G10	−22.6	16.4	−73.3	28.5
A5	17.2	16.4	−56.7	62.7
A36	49.0	10.5	3.6	82.1
m^{7}G46	106.6	39.3	42.0	194.4
A76	122.4	39.7	41.6	182.9
A9	166.3	19.3	121.6	217.5

[a] All values in degrees.

Since there are 76 riboses in tRNA^{Phe}, and since we have saved sets of atomic coordinates at invervals of 0.005 ps, the 24-ps simulation provides a data base of 364 800 ribose structures that could be analyzed. To reduce the size of this data set and to eliminate much of the overlap in the data, we have chosen a representative subset of the structures. This reduced data base is composed of 4800 ribose structures, 800 for each of six riboses, taken at intervals of 0.03 ps and with the riboses chosen so that the widest possible range of sugar puckers was covered (Table I). All of these riboses are in purines, so that any possible subtle effects due to differences between purine riboses and pyrimidine riboses would be avoided. The northern hemisphere is well covered by riboses 10, 5, and 36, which fluctuate about the C2′-exo, C3′-endo, and C4′-exo configurations, respectively; the transition region (C4′-exo, O4′-endo, and C1′-exo) is spanned by riboses 46 and 76, both of which spontaneously pass from the southern to the northern hemisphere; and ribose 9 was chosen to examine the southern hemisphere, since it covers the C1′-exo, C2′-endo, and C3′-exo regions.

It should be emphasized that these structures all occur spontaneously during the simulation, since only the usual potential energy terms (bond stretching, bond angle deformations, torsional rotations about single bonds, van der Waals interactions, electrostatic interactions, and hydrogen bond stretching) are included in the potential function. No terms were added to explicitly represent sugar pucker energies or to bias the conformation of the ribose rings. All structures were generated by the molecular dynamics simulation, and they were not refined or altered in any way during the analysis. The resulting scatter in the data should therefore represent the kinds of thermal fluctuations that occur at 303.7 K, the mean temperature of the simulation.

Results and Discussion

Kinetics. Figure 1 shows the time course of the sugar pucker angle P for each of the six riboses of Table I over the 24 ps covered by the molecular dynamics simulation. The first four panels show behavior that is typical of all 76 riboses of tRNA^{Phe} except for two (riboses 46 and 76, shown in the last two panels of Figure 1). With those two exceptions, none of the riboses reaches the top of the O4′-endo barrier at $P = 90°$. All the other sugar puckers fluctuate over fairly narrow ranges, with occasional drifts, but remain in either the northern or southern quadrant. When repuckering, defined as crossing the O4′-endo barrier, does occur, it requires only a few picoseconds. A similar result has been described in the spontaneous repuckering of deoxyriboses in a DNA molecular dynamics simulation.[20]

We can get a very rough estimate of the frequency of repuckering if we assume that the various riboses in the simulation

(18) Jeffrey, G. A.; Taylor, R. *Carbohydr. Res.* **1980**, *81*, 182–183.
(19) Dunitz, J. D. *Tetrahedron* **1972**, *28*, 5459–5467.
(20) Singh, U. C.; Weiner, S. J.; Kollman, P. *Proc. Natl. Acad. Sci. U.S.A.* **1985**, *82*, 755–759.

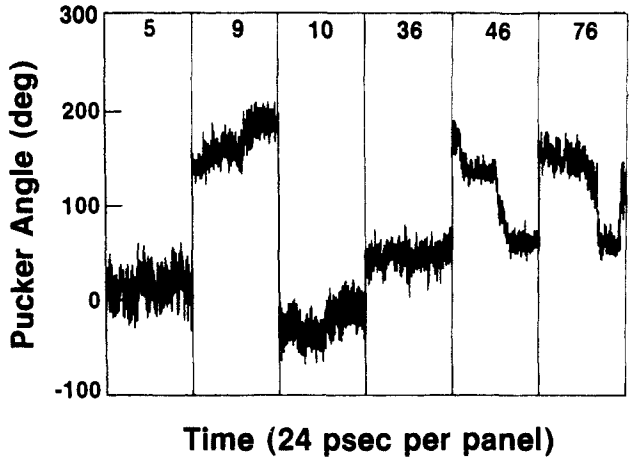

Figure 1. Time dependence of the pucker phase angle P(AS) for the six riboses used in this study. One panel contains the history of P vs. t for a single ribose, with the width of each panel corresponding to 24 ps. The identity of the ribose is indicated by the number at the top of the panel. The statistical properties of each pucker angle are summarized in Table I.

are, to a first approximation, independent of one another, so that the 24-ps simulation of a molecule with 76 riboses is equivalent to a simulation on one ribose lasting 76 × 24 ps = 1.8 ns. Between one and three repuckerings are observed during that time, depending on how one scores the behavior of ribose 76, which is still near the O4′-endo configuration at the end of the simulation. Consequently, repuckering occurs at intervals on the order of 0.5–2 ns. A similar calculation on the 80-ps in vacuo simulation of a DNA with 10 deoxyriboses, where two sugars spend at least some of their time in the N and S configurations,[20] produces a similar estimate, with one repuckering every 0.4 ns. We note that none of the sugars that repucker is in a double-stranded region, either in the tRNA simulation or in the DNA simulation, from which we conclude that repuckering will be more frequent in single-stranded regions, loop regions, and at the terminal residues of double helical molecules. This is, of course, to be expected, but the combined results of these simulations suggest that there would be at least an order of magnitude of difference in the frequency of repuckering in double-stranded regions as opposed to other regions.

Comparison of Formalisms. The AS and RWS methods define the amplitude of puckering in terms of the maximum deviation of ring torsion angles from the cis conformation. The CP description measures amplitude in terms of the maximum reached by individual atoms in their excursions away from the ring plane. There are differences between the values of P defined by the three formalisms (eq 2, 4, and 6), although these differences are generally believed to be rather small.[5,18] Our data base allows an examination of those variations, and Figure 2 presents a plot of P(CP) vs. P(AS). Not surprisingly, the deviation from a linear relationship is found to be a periodic function of P (Figure 2a). If P is expressed in degrees, the following empirical relationship describes the data of Figure 2a quite well:

$$P_{CP} = P_{AS} - 4 \sin (2P_{AS}) \quad (8)$$

The data are scattered in a band about the line predicted by eq 8, the band having a half-width of about 2°. When the systematic variation (eq 8) and the random scatter are added together (Figure 2b), the maximum difference between P(CP) and P(AS) is on the order of 6°, which is about twice the difference previously reported.[5,18] If one is looking at the fine details of sugar pucker, attempting, for example, to distinguish between envelope (E) and twist (T) configurations, a difference of 6° between values of P(CP) and P(AS) could be large enough to lead to results that depend on which formalism is used, since neighboring E and T configurations are separated by only 18°. We have also examined a plot of P(RWS) vs. P(AS), and we find that differences between these two formalisms, both of which define sugar pucker in terms

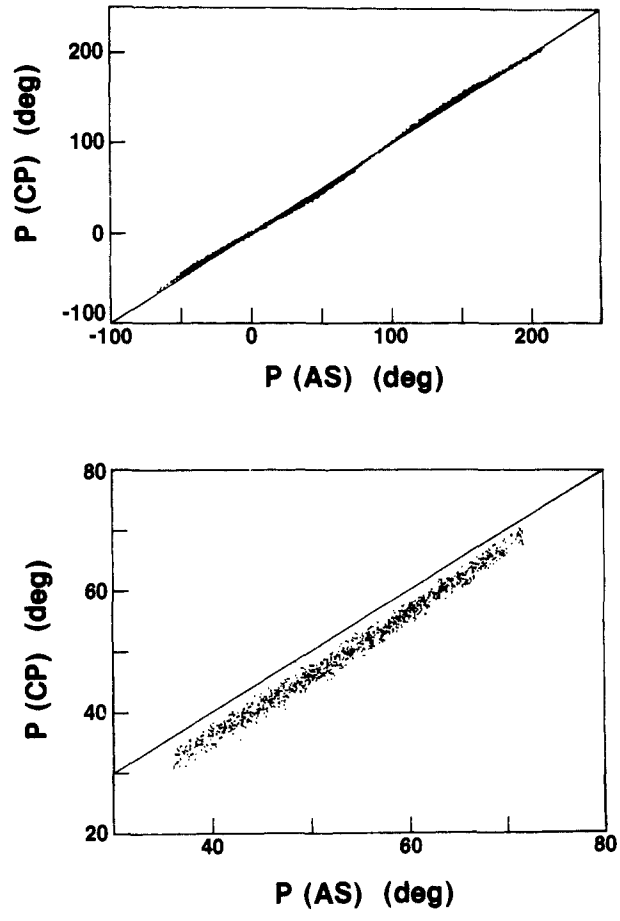

Figure 2. Relationship between the Altona-Sundaralingam and the Cremer-Pople definitions of pucker phase angle. Each of the 4800 structures is represented by a single point in the upper panel (a), which spans the entire data set. The lower panel (b) shows the data over the range 36° ≤ P < 72°, corresponding to all structures in the C4′-exo conformation. The solid line in both panels represents the equation: P(CP) = P(AS). The data in this figure are better described by the relationship of eq 8.

of torsions, are negligible. Finally, the plot of P(CP) vs. P(RWS) is virtually identical with the plot of P(CP) vs. P(AS).

Regarding amplitudes, we find that a plot of the RWS amplitude vs. the AS amplitude is linear, as expected, but the slope is not 1.00; the best fit gives θ_m(RWS) = 1.03θ_m(AS). At intermediate amplitudes, around 40°, the RWS amplitudes are confined within a band of width ±2° on either side of that line.

Dunitz[19] has presented a relationship between θ_m(RWS) and q(CP), which, for small puckering amplitudes, is given by eq 7. For larger puckering amplitudes, he suggested that a proportionality constant of 94.9 should be used in place of the factor of 102.5 in eq 7, but eq 7 is in good agreement with results from a variety of crystallographic structures.[5] When we plot θ_m(RWS) vs. q(CP), we obtain data which scatter about a straight line with a slope of 105.5 (not shown). Many workers have assumed that eq 7 will apply to θ_m defined by either the AS or RWS formalisms, and because of the 3% difference in these (previous paragraph), a plot of θ_m(AS) vs. q(CP) follows the relationship of eq 7 very closely (Figure 3). The average ratio between these two amplitudes is 102.9.

From the scatter in Figures 2 and 3, it is evident that at a given point in (P,θ_m) space there will be many slightly different ribose structures. In the introduction, we raised the question of how large the fluctuations are in bond lengths, bond angles, and endocyclic torsions at a given value of pucker angle and amplitude. We will examine that issue in the next section, after we have looked at the variations of mean values of some of those parameters along the pseudorotation pathway.

Pseudorotation Pathway. In the few cases of spontaneous repuckering of sugars in molecular dynamics simulations, passage

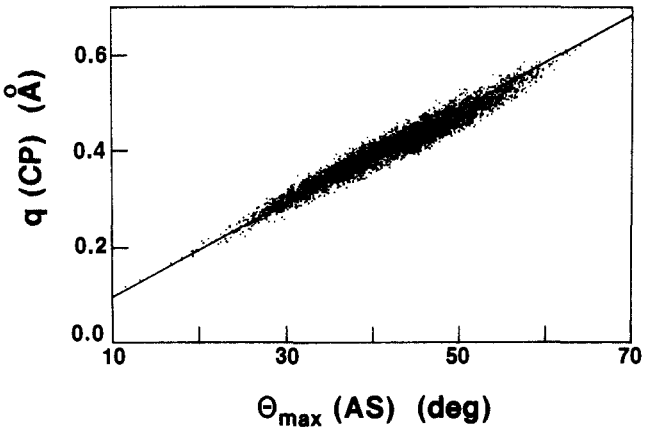

Figure 3. Relationship between the Altona–Sundaralingam and the Cremer–Pople definitions of pucker amplitude. All 4800 structures are represented. The solid line represents the Dunitz equation[19] (eq 7).

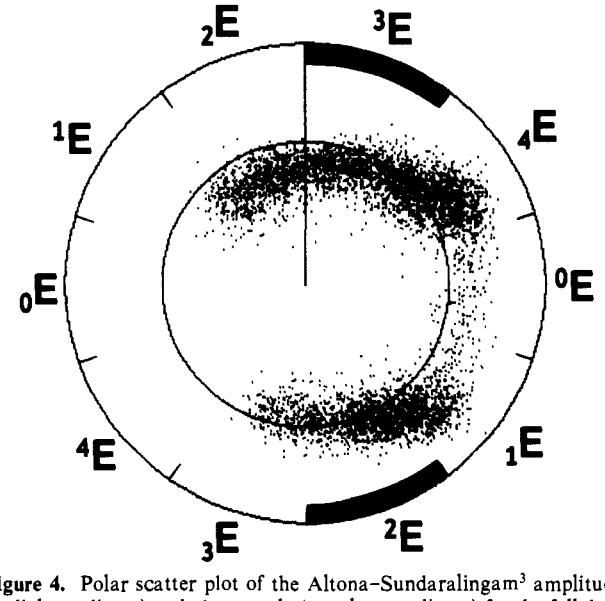

Figure 4. Polar scatter plot of the Altona–Sundaralingam[3] amplitude (radial coordinate) and phase angle (angular coordinate) for the full data set. The outer circle corresponds to θ_m = 70°, while the inner circle represents the average amplitude of all 4800 ribose structures, θ_m = 41.8°. The plot is divided into segments that cover the 10 envelope configurations, with the two regions that are traditionally regarded as energy minima indicated by the dark bands. ^{2}E = C2′-endo, $_2$E = C2′-exo, ^{0}E = O4′-endo, etc.

between the N and the S hemispheres has always been observed to proceed via the E pathway,[15,20] avoiding the O4′-exo region near P = 270° (Figure 1). If the pseudorotation pathway is indeed followed, we would expect the amplitude to be essentially constant. Figure 4 shows a polar scatter plot of the 4800 ribose structures of our tRNA data base. The average pucker amplitude of these structures is 41.8°, represented by the inner circle in the figure. There are clear deviations from the pseudorotation pathway, with large average amplitudes observed in the O4′-endo region and particularly small average amplitudes in the C2′-exo region. The latter is in keeping with the prediction, based on the (P,θ_m) conformational energy map of Levitt and Warshel,[6] that riboses attempting to cross the O4′-exo barrier would find the pass through the high-energy western region of the map at a very small amplitude, around θ_m = 20°. In contrast with Levitt and Warshel,[6] however, we find passage over the eastern O4′-endo barrier to occur at amplitudes around 50°, rather than around 35°, which their map predicts. The very high amplitudes which occasionally occur (Figures 3 and 4) are somewhat unexpected, since the Levitt–Warshel map indicates energies in excess of 5 kcal/mol for such structures.

When we consider the principal results of the previous paragraph—the deviations from the circular pseudorotation pathway and the broad range of observed amplitudes—we must ask whether there is experimental evidence to support these ideas, so that they are not just artifacts of the potential function used in the simulation. The best data against which to test these results are from the tRNA^{Phe} crystal structure,[21] from which the simulation was started. Figure 5 shows a (P,θ_m) plot similar to Figure 4, but with the 76 ribose conformations from the crystal structure. Since none of those sugar puckers lies in the eastern quadrant, we have added 24 points corresponding to the *deoxy*ribose puckers found in the crystal structure of a DNA dodecamer.[22] Although the collection of experimental points is not very large, there is enough similarity between Figures 4 and 5 to suggest that the (P,θ_m) distribution of the molecular dynamics data base is reasonable.

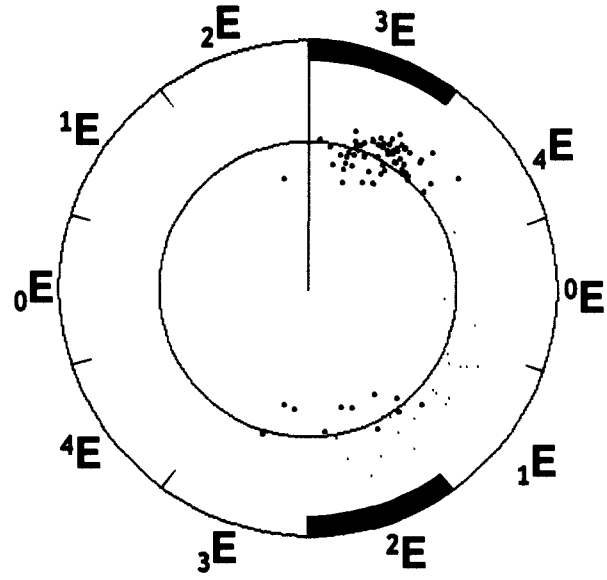

Figure 5. Polar scatter plot of the 76 crystallographic ribose structures of tRNA^{Phe}, from the coordinates of Hingerty et al.[21] (heavy points). For comparison, and to provide a few data points in the eastern quadrant, the *deoxy*ribose structure of the Dickerson dodecamer[22] are also indicated (light points). This figure is drawn to the same scale as Figure 4.

In the AS formalism, it is assumed that two independent variables, P and θ_m, are sufficient to describe the relationship between the five endocyclic torsion angles (eq 1). Although the torsions are mutually constrained by the condition of ring closure, the flexibility of bonds and valence angles causes eq 1 to be only an approximation. This is illustrated in Figure 6, a scatter plot of θ_1 vs. P. Part of the variation is due to the dependence of θ_m on P (Figure 4), and part is due to the flexibility of the covalent bonds and valence angles. Similar behavior is observed in the other endocyclic torsions. Deviations from eq 1 were also observed in a study of ribose puckering that used constrained energy minimization.[6]

There is an obvious and important relationship between sugar pucker and backbone conformation, since the exocyclic torsion δ and the endocyclic torsion θ_1 both describe rotations about the C3′–C4′ bond. The predicted and observed relationships are compared in Figure 7. In contrast with Figure 6, the scatter is relatively uniform and independent of P. The nonuniformities in Figure 6 are probably a consequence of the fact that P(AS) is *defined* in terms of θ_1.

It has been argued by Westhof and Sundaralingam[23] that there is a dependence of backbone flexibility on sugar pucker, for the following reason. Changes in P produce larger changes in δ when the sugar pucker is in the southern quadrant than they do when it is in the northern quadrant, since the slope in Figure 7 is steeper

(21) Hingerty, B.; Brown, R. S.; Jack, A. *J. Mol. Biol.* **1978**, *124*, 523–534.
(22) Fratini, A. V.; Kopka, M. L.; Drew, H. R.; Dickerson, R. E. *J. Biol. Chem.* **1982**, *257*, 14686–14707.
(23) Westhof, E.; Sundaralingam, M. *J. Am. Chem. Soc.* **1983**, *105*, 970–976.

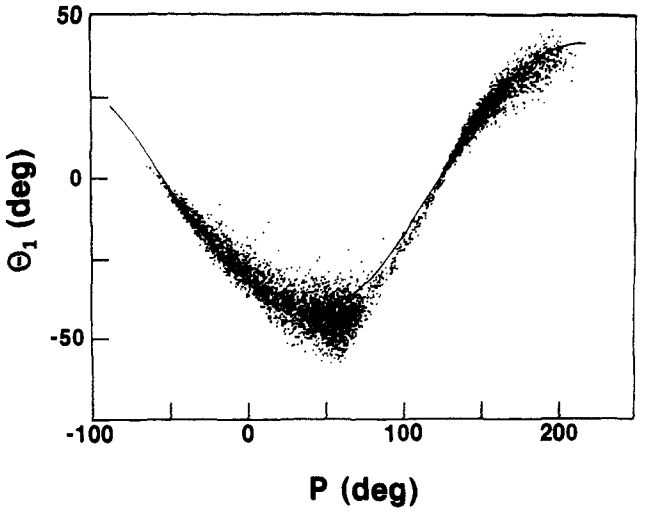

Figure 6. Scatter plot showing the relationship between the endocyclic torsion θ_1 (C2′–C3′–C4′–O4′) and the pucker phase angle. Each of the 4800 ribose structures is represented by a single point, while the solid line indicates the relationship of eq 1.

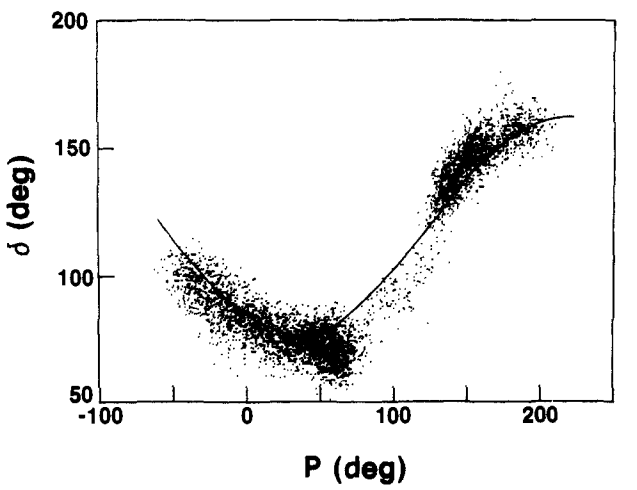

Figure 7. Scatter plot showing the relationship between the exocyclic torsion δ (O3′–C3′–C4′–C5′) and the pucker phase angle. Each structure of the full data set is represented by a point, and the solid line was generated by combining eq 1 with the observation that, for ideal tetrahedral geometry at the C3′ and C4′ carbons, it would be expected that $\delta = \theta_1 + 120°$.

at values of P in the range 120–180° than it is when P is in the range 0–60°. While such an argument is logical from the standpoint of idealized pseudorotation behavior, the substantial thermal fluctuations in the value of δ at any given value of P (Figure 7) are sufficient to seriously diminish any effects of pucker-dependent backbone flexibility.

Another prediction of theoretical studies,[7] analysis of crystallographic structures,[7,24] and constrained energy minimization studies[11] is that there is a periodic dependence of valence angles on P. We do find such behavior, and the case of a typical angle within the ribose ring is shown in Figure 8. Although the thermal fluctuations are large enough that they would be expected to swamp the effects of the predicted variations, which are of very small amplitude, we actually observe a systematic dependence of the valence angle on P that is several times larger than that of any of the earlier studies.[7,11,24] We also observe a dependence of valence angles on θ_m that is qualitatively similar to that predicted by Westhof and Sundaralingam,[7] so their relationship is correct for energy-minimized structures, crystallographic structures, and thermally averaged structures, but again we observe very large

(24) Murray-Rust, P.; Motherwell, S. *Acta Crystallogr., Sect. B: Struct. Sci.* **1978**, *34*, 2534–2546.

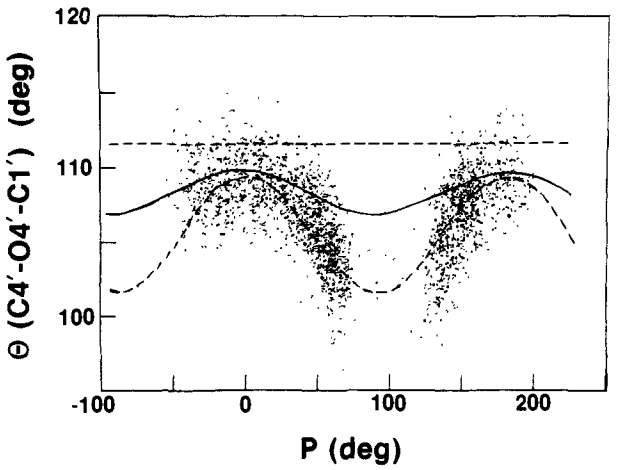

Figure 8. Scatter plot showing the dependence of the endocylcic valence angle C4′–O4′–C1′ on pucker phase angle. Each of the 4800 ribose structures is represented by a point. The pucker dependence predicted by Westhof and Sundaralingam[7] is shown for a puckering amplitude of $\theta_m = 20°$ (upper dashed line) and for $\theta_m = 60°$ (lower dashed line). Although nearly all the structures fall within that range of θ_m (see Figure 3), the thermal fluctuations in this valence angle are clearly much larger than predicted by Westhof and Sundaralingam. The solid line indicates the pucker dependence predicted by Olson.[11]

thermal scatter in the data (not shown). We believe that these large variations in valence angle are probably real; energy minimization (which is also used in crystallographic structure refinement) will tend to produce valence angles whose values are near to their "ideal" values, because of the very strong force constants. At the same time, even large force constants, on the order of 100 kcal/(mol·rad^2), allow root-mean-square thermal fluctuations of about 4° in valence angles during dynamic simulations, and deformations up to 8° are not prohibited when these are required by strains such as those associated with ring repuckering.

Energetics. Previous studies[6,11,12] did not agree on the height of the repuckering barrier near the O4′-endo configurations, nor did they agree on which components of the energy are primarily responsible for that barrier. The position of Levitt and Warshel,[6] that pseudorotation is relatively free, with an energy barrier of only 0.5 kcal/mol, is a minority opinion.[7,10,12] (See ref 10 for an extensive discussion and for the further references.) Levitt and Warshel[6] concluded that the contributions from deforming bond angles and from nonbonded interactions were relatively independent of P, and that the principal contribution to the barrier is the component due to torsional rotations. While Olson[11] agreed that this latter contribution is substantial, she found that the principal contribution to the barrier was that due to nonbonded interactions; she also found that the bond angle component is not flat but has a valley at the O4′-endo conformation. We suspect that these differences are primarily due to differences in the conformations that were generated during energy minimization by the combination of different starting geometries and different parameters in the potential functions. Since molecular dynamics generates hundreds of configurations for each region of puckering space, we have examined the dependence of each of the components of the energy on P by averaging over those configurations.

The total energy of the ribose is calculated by considering the structure defined by the five atoms in the furanose ring and the four substituent atoms (C5′, O3′, O2′, and the purine N9). For this structure, the total energy is calculated for the stretching of the 9 bonds, the deformation of the 13 valence angles, the nonbonded interactions, and rotations about bonds (torsions). The number of torsions to be included is discussed in the following paragraph.

One of the questions that arises in establishing the potential energy function of a complex molecule is how to properly treat rotations about the bond between two atoms when both of them have two or three other heavy atoms (nonhydrogens) as sub-

Table II. Torsions in Riboses (Purines)

	included in this study	gauche potential ribose	gauche potential deoxyribose
Endocyclic Torsions			
O4′-C1′-C2′-C3′		X	X
C1′-C2′-C3′-C4′	X		
C2′-C3′-C4′-O4′		X	X
C3′-C4′-O4′-C1′			
C4′-O4′-C1′-C2′	X		
Exocyclic Torsions			
N9-C1′-C2′-O2′		X	
O2′-C2′-C3′-O3′	X	X	
O3′-C3′-C4′-C5′	X	X	X
Mixed Torsions			
O4′-C1′-C2′-O2′		X	
N9-C1′-C2′-C3′	X		
C1′-C2′-C3′-O3′		X	X
O2′-C2′-C3′-C4′	X	X	
C2′-C3′-C4′-C5′	X		
O3′-C3′-C4′-O4′		X	X
C5′-C4′-O4′-C1′	X		
C4′-O4′-C1′-N9	X		

stituents. Consider, for example, the bond between the C3′ and C4′ atoms of a ribose ring. Each of these has two other heavy atoms bonded to it, C2′ and O3′ for the former and C5′ and O4′ for the latter. How should the C3′–C4′ torsion be identifed? One way would be to choose any two appropriate substituent atoms; if, for example, we choose the endocyclic definition for the torsion, it would be designated C2′–C3′–C4′–O4′. The positions of the other atoms (O3′ and C5′) can then be constrained by appropriate combinations of energies for deforming bond angles and by the use of "improper torsions"[25] that maintain chirality about C3′ and C4′. The possible disadvantage of this method is that not all substituent atoms are treated alike, so an alternative procedure is to include all four definitions for the torsion in the potential function (C2′–C3′–C4′–O4′; C2′–C3′–C4′–C5′; O3′–C3′–C4′–O4′; O3′–C3′–C4′–C5′), with appropriate adjustments in the values of the torsional force constants. A variety of methods for defining torsions has been used by other investigators in molecular modeling studies on proteins and nucleic acids. In our own case, we considered this issue in setting up our first study on tRNA bending,[26] and we chose a compromise position that treats neither the minimum set of five endocyclic ribose torsions nor the maximum set of all 16 possible ribose torsions (Table II). The nine torsions chosen for the bending studies[26,27] were also used in our molecular dynamics simulations.[13-16]

The dependence of the total internal energy of the ribose on pucker phase angle is shown in Figure 9. At a given pucker angle, substantial fluctuations in energy are evident, with root-mean-square deviations of about 2.5 kcal/mol. This is the size of energy fluctuations to be expected for a ribose with the substituent atoms included.[28] There is an appropriate small difference between the energy minima in the northern and southern quadrants (0.4 kcal/mol), and the height of the barrier (about 1.5 kcal/mol) agrees with values in the range 1.3–2.0 kcal/mol given by Olson[11] and by Weiner et al.;[12] our value is three times that of Levitt and Warshel.[6] Our barrier height is about one-third the experimental value,[8,9] but it must be remembered that this calculation gives potential energy only, while the experimental result is a free energy. The largest contribution to the barrier, in this simulation, is the torsional energy, with the energy of deforming bond angles being of secondary importance.

We have examined possible modifications to the potential function. Results of these modifications have to be considered

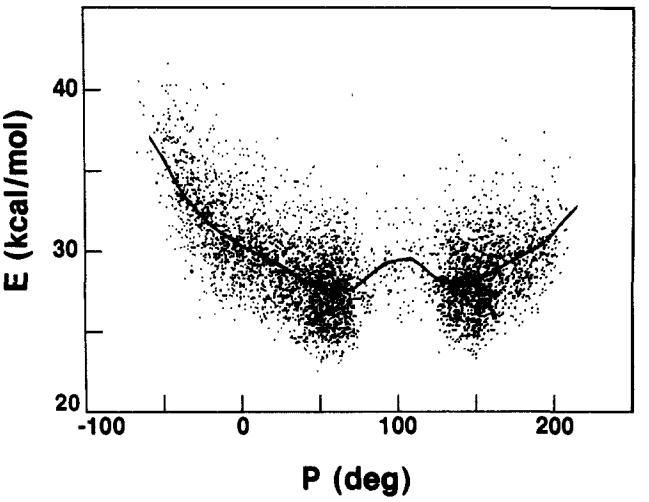

Figure 9. Total conformational energy as a function of pucker phase angle. Each point represents one of the 4800 ribose structures. The solid line connects the average energies for successive ranges of configurations. For example, the point at $P = 90°$ represents the O4′-endo conformation and covers the range $81° \leq P < 99°$. The next segment ($99° \leq P < 117°$) represents the O4′-C1′ twist conformation, and the point is plotted at $P = 108°$.

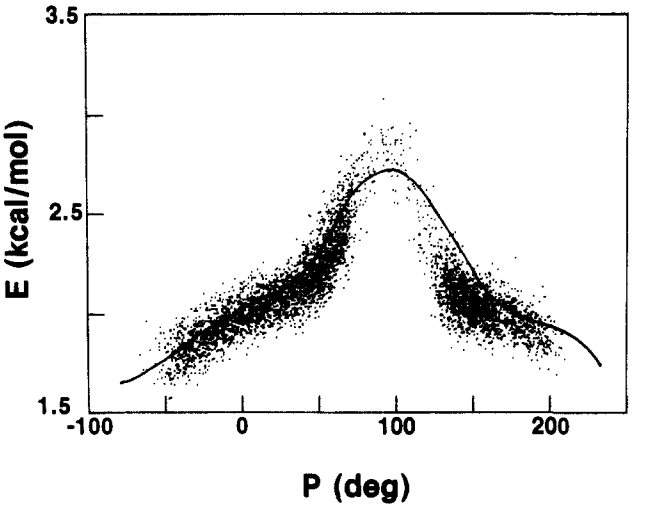

Figure 10. Pucker dependence of the gauche potential for ribose. The energies have been calculated using the set of nine torsions indicated in Table II and the potential parameters of Olson.[11] Points represent configurations from our molecular dynamics data set, while the solid line is the result obtained in Olson's energy minimization study.[11]

with a grain of salt, however, because they are based on energies calculated for modified potentials that are applied post hoc to our data set of 4800 structures, a set that was spontaneously generated during a simulation with an unmodified potential. We do not know how different our results would be if new simulations were run based on the modified potentials. (Such simulations are now being carried out in our laboratory).

The propensity of torsions containing terminal oxygens with unshared p electrons to adopt gauche rather than trans configurations is a well-established fact in small molecules, and it apparently persists in furanose rings (see ref 11 for a more extensive discussion). Olson[11] proposed a twofold torsional gauche term in the potential function for riboses. This term will, when used in combination with the standard threefold torsional potential, reproduce the experimental trans/gauche energy difference. When we use her barrier heights of 0.2 and 1.0 kcal/mol for O–C–C–C and O–C–C–O torsions, respectively, and calculate the energy of the gauche potential for the nine appropriate torsions (Table II) using our set of structures, we get a curve that shows the same qualitative dependence on pucker angle as Olson reported in her energy minimization studies, although our barrier height is about

(25) Brooks, B. R.; Bruccoleri, R. E.; Olafson, B. D.; States, D. J.; Swaminathan, S.; Karplus, M. *J. Comput. Chem.* **1983**, *4*, 187–217.
(26) Harvey, S. C.; McCammon, J. A. *Nature (London)* **1981**, *294*, 286–287.
(27) Tung, C. S.; Harvey, S. C.; McCammon, J. A. *Biopolymers* **1984**, *23*, 2173–2193.
(28) Cooper, A. *Prog. Biophys. Mol. Biol.* **1984**, *44*, 181–214.

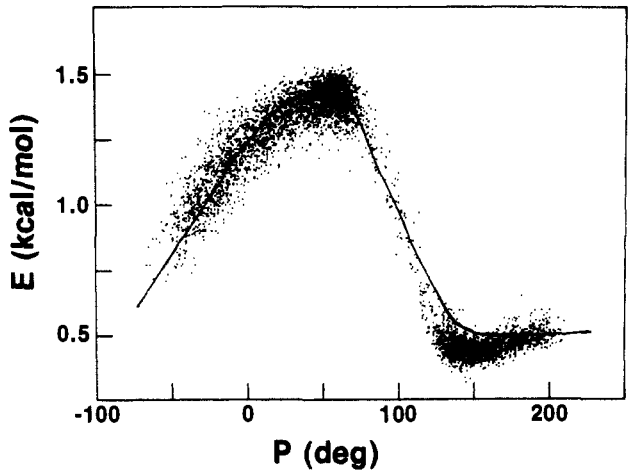

Figure 11. Pucker dependence of the gauche potential for deoxyribose, calculated using the set of five torsions indicated in Table II. See Figure 10 for further explanation.

0.2 kcal/mol higher than hers (Figure 10). If we consider only the five torsions that would be found in deoxyribose (Table II), the resulting gauche potential curve (Figure 11) is nearly identical with Olson's. Clearly, the gauche potential can be used to shift the relative energies of the C2′-endo and C3′-endo configurations in deoxyribose by about 0.5 kcal/mol, or to adjust the height of the barrier at O4′-endo, as proposed.[11]

Of course, it is free energy differences, rather than differences in potential energy, that determine the range and pathways of structural dynamics. At least two methods can be used to estimate free energies from molecular dynamics simulations. The quasi-harmonic approximation[29,30] evaluates the configurational entropy by carrying out a normal mode analysis on a model whose mean-square fluctuations are equal to those produced by molecular dynamics. Alternatively, one can determine the potential of mean force from the probability distribution function produced by the molecular dynamics simulation, using a restraining "umbrella sampling" potential to sample high-energy regions of conformational space if necessary.[31,32] The latter approach would be the most straightforward in the present case. Unfortunately, we cannot determine the potential of mean force as a function of pucker angle from our data set of 4800 structures, because the riboses which were used were selected specifically to cover pucker space, because each ribose is subject to external forces that bias its pucker, and because the 24-ps simulation is not long enough to generate an equilibrium probability distribution.

We have begun a series of molecular dynamics simulations to examine the effects of different potential functions on structures, dynamics, and energetics, beginning with 200-ps simulation of a single ribose, using the same potential function as was used in the present study. Figure 12 shows the pucker dependence of the potential of mean force and the potential energy, determined from that simulation. The potential of mean force has a large entropic component at the extreme values of pucker ($P < 0°$ and $P > 180°$). The potential energy curve is similar to that of Figure 9 except at the extremes ($P < 0°$ and $P > 180°$). Evidently, the riboses that reach these extremes in the tRNA simulation do so as a consequence of external stresses. Their structures are consequently somewhat different from those of the free ribose simulation, so the potential energy curve of Figure 9 does not reflect the intrinsic behavior of free riboses in this extreme region of configuration space. This result emphasizes the need for caution in extrapolating results from small molecule studies to those where the structure of interest is part of a large molecule, and vice versa.

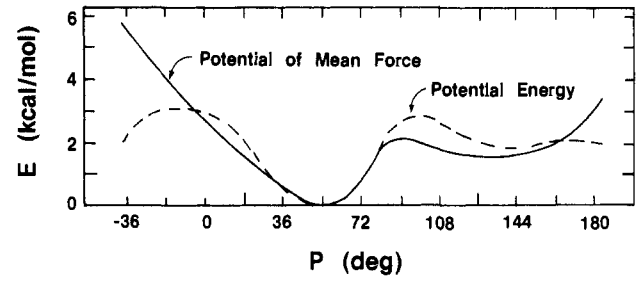

Figure 12. Potential energy and potential of mean force for ribose using our tRNA potential function; 50000 structures were selected from a 200-ps molecular dynamics simulation. The average potential energy was calculated for all structures in each of 20 windows of pucker phase angle, each window spanning 18°. The potential of mean force is determined from the observed probability distribution.[31,32]

On the other hand, the structural results shown in Figures 1–8 and the conclusions drawn from them are validated by calculations on the set of structures generated in the free ribose simulation; the results of the tRNA simulation and the single ribose simulation are essentially identical with regard to those issues. In particular, the free energy calculations reproduce the depence of amplitude on pucker shown in Figure 4.

Conclusions

The enormous data base generated by a molecular dynamics simulation provides an excellent perspective from which to examine structural, dynamic, and energetic questions. The sheer number of structures that are produced (thousands of ribose configurations in the present study) and the fact that they are a representative subset of all thermally accessible conformations make molecular dynamics a very powerful method for investigating conformational issues and for examining alternative parameters for the potential energy function.

Here we have taken advantage of the wide range of ribose puckers in $tRNA^{Phe}$ and of the spontaneous repuckering of two of them to examine the pseudorotation formalism, to investigate the structural and dynamic aspects of repuckering, and to check how well our potential energy function reproduces the experimental dependence of conformational energy on sugar pucker.

The conformational changes of repuckering are generally well described by the pseudorotation pathway. Transitions between the northern and southern quadrants do go through the eastern, rather than the western quadrant, as expected, and polar (P,θ_m) scatter plots show all observed conformations within a roughly circular band; both of these observations are consistent with the predictions of the pseudorotation formalism.[3] There are, however, two observations that are slightly at variance with the traditional concept of pseudorotation. First, at a given pucker angle there are very large fluctuations in puckering amplitude, both in the dynamic simulation (Figure 4) and in the crystallographic studies (Figure 5). Second, there is a substantial dependence of the average amplitude on pucker angle, with a smaller puckering amplitude in the region of the western barrier (O4′-exo) and a larger amplitude during passage over the eastern barrier (O4′-endo). This dependence was first predicted by Levitt and Warshel.[6]

When the three different formalisms[3-5] are compared, only small differences are found between them, and the deviations from ring planarity can be described either in terms of torsional angles[3,5] or in terms of atom distances from a reference plane.[4] Equation 7, first proposed by Dunitz,[19] is indeed found to describe the relationship between the torsional amplitude and the mean atomic displacement. This is shown in the plot of θ_m(AS) vs. q(CP) in Figure 3. We have also found a simple relationship between the two definitions of pucker phase angle, P(AS) and P(CP); that relationship is given by eq 8 and the data are shown in Figure 2.

In considering alternative sets of energy parameters for dynamics studies, we have found the most profound changes in the shape of the conformational energy curve (E vs. P) are produced

(29) Karplus, M.; Kushick, J. N. *Macromolecules* **1981**, *14*, 325–332.
(30) Levy, R. M.; Karplus, M.; Kushick, J.; Perahia, D. *Macromolecules* **1984**, *17*, 1370–1374.
(31) Torrie, G. M.; Valleau, J. P. *J. Comput. Phys.* **1977**, *23*, 187–199.
(32) Northrup, S. H.; Pear, M. R.; Lee, C. Y.; McCammon, J. A.; Karplus, M. *Proc. Natl. Acad. Sci. U.S.A.* **1982**, *79*, 4035–4039.

by changes in the torsional potential term. Of primary importance is the selection of which torsions are included and which are excluded when there are multiple definitions for rotations about a particular bond. For any particular problem, various combinations of those definitions and various values of the rotational barrier heights can be used to search for the optimum overall potential. The gauche effect in O-C-C-O and O-C-C-C torsions can be used to fine tune the total potential and may be important in the differences between ribose and deoxyribose rings.[11]

Although Figures 9 and 12 indicate that our potential energy function is reasonable, it does not exactly reproduce the locations of the energy minima that are predicted from the combined results of crystallographic and NMR studies[10] and of other theoretical studies.[6,11,12] For example, our minimum energy configuration is at C4′-exo rather than C3′-endo, and the second minimum is at C1′-exo rather than C2′-endo. Further refinement of the potential is needed. Since a variety of methods[29-32] can be used to determine free energy differences, rather than just differences in internal energy, we believe that appropriate simulations would provide a very useful comparison of the various potential functions used to model ribose structure and dynamics. Such studies are now underway in this laboratory.

Acknowledgments. We thank Eric Westhof for comments on a preliminary version of this paper. This research was supported by grants from the National Science Foundation (PCM-84-17001) and the National Institutes of Health (GM-34015).

(33) **Note Added in Proof**: It has come to our attention that a relationship between P(CP) and P(AS) identical with eq 8 (except with an amplitude of 3°, rather than 4°) has been reported previously (de Leeuw, H. P. M., et al. *Isr. J. Chem.* **1980**, *20*, 108-126). Also, we should have mentioned two refinements to the Altona-Sundaralingam method: First, there is an averaging procedure[3,17] that eliminates the problems of choosing a reference atom described in our discussion following eq 2. With this procedure, "there is no difference between the AS and RWS results, except for roundoff errors" (Altona, C., personal communication). Second, eq 1 can be improved by the addition of a small phase angle ϵ_j (always less than 1.5° for ribose) and multiplication of θ_j by an amplitude factor a_j (ranging from 0.977 to 1.016 for ribose); values of the parameters and a full discussion are given by de Leeuw in the following: de Leeuw, F. A. M., et al. *J. Mol. Struct.* **1984**, *125*, 67-88.

Mechanism of Carbonyl Insertion Reaction of Pd and Pt Complexes. An ab Initio MO Study

Nobuaki Koga and Keiji Morokuma*

Contribution from the Institute for Molecular Science, Myodaiji, Okazaki, 444 Japan.
Received April 1, 1986

Abstract: The carbonyl insertion reaction of $Pd(CH_3)(H)(CO)(PH_3)$, **1**, and $Pt(CH_3)(H)(CO)(PH_3)$, **3**, has been studied by means of the ab initio MO method with the energy gradient. The transition state has been determined for the reaction of both **1** and **3**, which shows unequivocally that the reaction proceeds via methyl group migration. The reaction of **1** has a lower activation energy and is less endothermic than that of **3**. These differences can be ascribed to the difference of M-CH_3, M-CO, and M-$COCH_3$ bond strengths between the Pd and the Pt complexes, those in the Pt complexes being stronger than in the Pd complexes. Substitution by an electron-withdrawing fluorine on the alkyl group makes the metal-alkyl bond stronger and the activation barrier higher. An electron-releasing methyl substitution gives a reverse effect. A stronger trans effect makes the metal-carbon bond weaker to give a lower activation barrier.

The carbonyl insertion reaction 1 is one of the most important elementary organometallic reactions. This reaction has been implicated in various catalytic cycles as one of the key steps.[1] Many experimental studies have been carried out for better understanding of this important reaction.[2,3]

$$M(R)(CO)(L)_n \rightarrow M(COR)(L)_m \qquad (1)$$

There are several questions to be answered about this reaction. One central concern about the reaction mechanism has been the question whether (i) it is the alkyl group that migrates to the carbonyl group or (ii) it is the carbonyl group that migrates to insert into the metal-alkyl bond. One of the most elegant studies

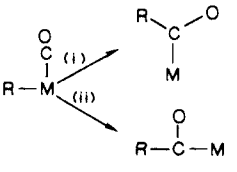

Scheme I

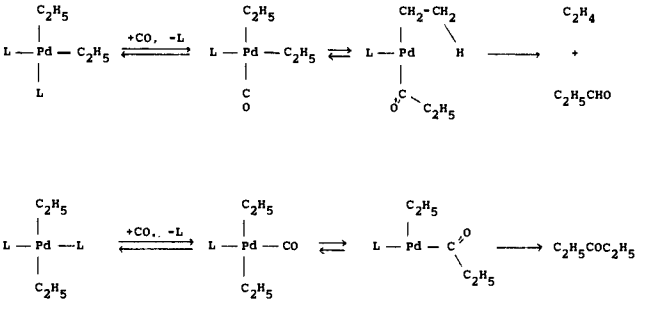

on this problem is that of $Mn(CH_3)(CO)_5$ by Noack and Calderazzo,[4] in which the reaction has been established to proceed via methyl group migration. In addition, the mechanism of carbonyl insertion reaction of rhodium,[5] iridium,[6] iron,[7] platinum,[8]

(1) See, for instance: Cotton, F. A.; Wilkinson, G. *Advanced Inorganic Chemistry*; Wiley: New York, 1980.
(2) Wojcicki, A. *Adv. Organomet. Chem.* **1973**, *11*, 87.
(3) (a) Calderazzo, F. *Angew. Chem., Int. Ed. Engl.* **1977**, *16*, 299. (b) Anderson, G. K.; Cross, R. J. *Acc. Chem. Res.* **1984**, *17*, 67.
(4) (a) Noack, K.; Calderazzo, F. *J. Organomet. Chem.* **1967**, *10*, 101. (b) Noack, K.; Ruch, M.; Calderazzo, F. *Inorg. Chem.* **1968**, *7*, 345. (c) Flood, T. C.; Jensen, J. E.; Statler, J. A. *J. Am. Chem. Soc.* **1981**, *103*, 4410.
(5) (a) Slack, D. A.; Egglestone, D. L.; Baird, M. C. *J. Organomet. Chem.* **1978**, *146*, 71. (b) Egglestone, D. L.; Baird, M. C.; Lock, C. J. L.; Turner, G. *J. Chem. Soc., Dalton Trans.* **1979**, 1576.
(6) Glyde, R. W.; Mawby, R. J. *Inorg. Chim. Acta.* **1971**, *5*, 317.

0002-7863/86/1508-6136$01.50/0